Blood-derived DNA methylation clusters associate with adverse social exposures and endophenotypes of stress-related psychiatric illness in a trauma-exposed cohort of women

Authors:
JR Pfeiffer[1,2], Sanne J.H. van Rooij[3], Yara Mekawi[4], Negar Fani[3], Tanja Jovanovic[5], Vasiliki Michopoulos[3], Alicia K. Smith[3,6], Jennifer S. Stevens[3], Monica Uddin[7]

Affiliations:
1. Department of Psychology, University of Illinois at Urbana-Champaign, Urbana, IL, USA
2. Carl R. Woese Institute for Genomic Biology, Urbana, IL, USA
3. Department of Psychiatry and Behavioral Sciences, Emory University School of Medicine, Atlanta, GA
4. University of Louisville, Department of Psychological and Brain Sciences, Louisville, KY
5. Department of Psychiatry and Behavioral Neurosciences, Wayne State University, Detroit, MI
6. Department of Gynecology and Obstetrics, Emory University School of Medicine, Atlanta, GA
7. Genomics Program, College of Public Health, University of South Florida, Tampa, FL, USA

Keywords:
Peripheral epigenetics, neuroimaging, adverse social environment, biological embedding, trauma

Corresponding author:
Address correspondence to:
Monica Uddin, PhD
University of South Florida
3720 Spectrum Blvd., Suite 304
813-974-9765
monica43@usf.edu

Manuscript details:
Words in abstract: 349
Words in text: 6846
Number of references: 127
Number of figures: 3
Number of tables: 4

Abstract

Adverse social exposures (ASEs) such as low income, low educational attainment, and childhood/adult trauma exposure are associated with variability in brain region measurements of grey matter volume (GMV), surface area (SA), and cortical thickness (CT). These CNS morphometries are associated with stress-related psychiatric illnesses and represent endophenotypes of stress-related psychiatric illness development. Epigenetic mechanisms, such as 5-methyl-cytosine (5mC), may contribute to the biological embedding of the environment but are understudied and not well understood. How 5mC relates to CNS endophenotypes of psychiatric illness is also unclear.

In 97 female, African American, trauma-exposed participants from the Grady Trauma Project, we examined the associations of childhood trauma burden (CTQ), adult trauma burden, low income and low education with blood-derived 5mC clusters and variability in brain region measurements in the amygdala, hippocampus and frontal cortex subregions. To elucidate whether peripheral 5mC indexes CNS endophenotypes of psychiatric illness, we tested whether 73 brain/blood correlated 5mC clusters, defined by networks of correlated 5mC probes measured on Illumina's HumanMethylation Epic Beadchip, mediated the relationship between ASEs and brain measurements.

CTQ was negatively associated with rostral middle frontal gyrus (RMFG) SA (β = - 0.231, p = 0.041). Low income and low education were also associated with SA or CT in a number of brain regions. Seven 5mC clusters were associated with CTQ (pmin = 0.002), two with low education (pmin = 0.010), and three with low income (pmin = 0.007). Two clusters fully mediated the relation between CTQ and RMFG SA, accounting for 47% and 35% of variability respectively. These clusters were enriched for probes falling in DNA regulatory regions, as well as signal transduction and immune signaling gene ontology functions. Methylome-network analyses showed enrichment of macrophage migration ($p = 9x10^{-8}$), T cell receptor complex ($p = 6x10^{-6}$), and chemokine-mediated signaling ($p = 7x10^{-4}$) pathway enrichment in association with CTQ.

Our results support prior work highlighting brain region variability associated with ASEs, while informing a peripheral inflammation-based epigenetic mechanism of biological embedding of such exposures. These findings could also serve to potentiate increased investigation of understudied populations at elevated risk for stress-related psychiatric illness development.

Introduction

Adverse social exposures (ASEs) such as low income, low educational attainment, childhood trauma, and adult trauma exposure, are common in the United States (US). Over the past five years, poverty rates in the US have ranged from 12 to 15%[1], and are likely to increase due to the impact of the COVID-19 pandemic[2]. The percentage of US adults aged 18 to 24 that finish high school with a diploma or GED is roughly 88%, meaning that over one million students per year leave high school without completion credentials[3]. Past year exposure to physical abuse in US children ranges from 4% to 16%, whereas past year psychological abuse is reported in 10% of children in the US; sexual abuse is experienced at some point during childhood in 15% to 30% of children[4]. Furthermore, in a US population-based study of 34,653 participants, researchers found that depending on self-reported race/ethnicity, respondents' prevalence of lifetime trauma exposure varied between 66% and 84%[5]. Other researchers have observed a lifetime traumatic exposure prevalence ranging from 50% to 90%[6-8]. ASEs are known to have long-term impact on emotional well-being and mental health; however, the mechanistic basis for these effects remain poorly understood.

One particularly salient risk following ASE exposure is the development of stress-related psychiatric illness or symptoms of such illnesses. For example, in both adults and children, poverty-related stress is associated with increased internalizing symptoms (e.g., sadness or anxiety), involuntary engagement stress responses (e.g., emotional arousal or intrusive thoughts), externalizing symptoms (e.g., acts of aggression or theft), and involuntary disengagement stress responses (e.g., emotional numbing or cognitive interference) [9]. Relatedly, World Health Organization (WHO) data has shown that rates of anxiety, mood, and substance-use disorders are all positively correlated with measures of socioeconomic disadvantage, including both low income and low educational attainment [10]. Moving a step beyond correlation, a longitudinal study found that higher educational attainment significantly attenuated both the overall risk of adult onset major depressive disorder (MDD), particularly in women, and the conditional risk of MDD as well[11].

The effects of childhood maltreatment or trauma on long-term mental health prognoses are also well-documented. In a recent meta-analysis of over 190 studies and 68,000 participants, researchers observed that higher childhood maltreatment (including potential traumas such as emotional abuse,

physical abuse, sexual abuse) scores were associated with MDD diagnosis later in life and with depression symptom severity[12]. This built upon previous work showing that exposure to any form of maltreatment during childhood was associated with a two-fold risk of MDD development, and nearly a three-fold risk of generalized anxiety disorder (GAD) development in adulthood[13]. Although childhood and adolescence are regarded as particularly vulnerable periods of development, the impact of trauma on psychiatric illness/symptom development are also notable when trauma is experienced in adulthood, with effects that are known to vary by race/ethnicity and gender. A particularly salient example of this is evident in the potential development of post-traumatic stress disorder (PTSD) after trauma. Recent population-based work highlights race/ethnic differences in psychiatric illness development and PTSD in particular. Researchers found that African Americans are generally more resilient to developing psychiatric illness after a TE, compared to other races/ethnicities[14]; however, this resilience does not apply to PTSD, where African Americans experience elevated conditional PTSD development rates relative to other races/ethnicities[14]. This, in tandem with research showing that females are subject to almost double the risk of developing PTSD and other mood-anxiety disorders throughout their lifetime[6, 15-17], highlights that African American women in particular may be subject to elevated risk of stress-related psychiatric illness development.

A great deal of work has been placed in identifying the neural correlates of poverty, low education, and childhood/adult trauma exposure. Researchers have identified specific signatures of central nervous system (CNS) variability in association with ASEs using methods such as structural magnetic resonance imaging (MRI) and functional MRI (fMRI). In rodent [18, 19] and human [20-24] studies, observed neural correlates of ASEs include variability in volumetric, cortical thickness (CT), surface area (SA), excitability, and connectivity measures. Brain regions including frontal cortex, hippocampus, and amygdala, contribute to adaptive behavioral and emotional responses, and are relevant to psychiatric illness development due to their contributions to the generation and regulation of major decision-making, memory formation, and stress-reactivity processes [25]. To this end, a meta-analytic study showed that frontal pole (FP), superior frontal gyrus (SFG), and rostral middle frontal gyrus (RMFG) frontal cortex subregions are heavily involved in attention, working memory, cognitive flexibility, and executive reasoning [26], with added involvement of the frontal pole in introspection and longitudinal thinking [27]. The anterior cingulate cortex (ACC) is

regarded as a mediator of the interactions between higher level cognitive processes and emotion/stress reactivity[28], and the orbito-frontal cortex (OFC) contributes to decision making and emotional processing functions[29]. These functions are impaired in numerous mental illnesses, including but not limited to PTSD[30], MDD[31], GAD[32], bipolar disorder[33], and schizophrenia[33]. These neural correlates of ASEs are associated with the development of stress-related psychiatric illnesses and may represent neural endophenotypes of said disorders[34-36].

Importantly though, the effects of ASEs do not travel directly from environment to psychiatric illness. The cascade of effect, rather, travel initially through the neuroendocrine system as a response to stressful external stimuli[37], whereby cortisol signaling occurs throughout the body, engaging immune (and other) biological networks[38]. This immune network activation and responses to cortisol signaling result in neural growth, inflammation, metabolism, and stress-related pathway disruption through epigenetic and other molecular mechanisms[39, 40]. The process of DNA methylation, which commonly refers to the addition of a 5-methyl-cytosine (5mC) residue to a cytosine-phosphate-guanine (CpG) base-pair, is one such epigenetic mechanism, and is understood to enhance or reduce mRNA transcription of genes in an experience-dependent, and temporally-stable manner[41]; continued research has pointed to the importance of 5mC in this biological embedding of external stimuli[42, 43]. Because of challenges in taking epigenetic measurements from a living human brain, the primary etiologic tissue of interest in regard to psychiatric illness development, peripheral tissues such as blood or saliva serve as proxies for etiological tissue. It is well-documented that these peripheral epigenetic measures can index changes to the hypothalamic-pituitary-adrenal (HPA)-axis [44, 45], immune system [46, 47], and CNS [48-50], although the direction of effect may be discordant across tissues [49, 51]. Stress-related physiological responses and their accompanying epigenetic alterations are thought to confer the biological embedding of ASEs [52, 53], and can ultimately increase the risk of stress-related psychiatric illness [39, 54]. Peripheral epigenetic measures can also index CNS-relevant endophenotypes of psychiatric illness development, as observed in studies using neuroimaging and peripheral epigenetic measures in tandem. However, these studied have primarily utilized candidate gene approaches, investigating 5mC in the *SLC6A4* [55-57], *NR3C1* [58, 59]], *FKBP5* [60], and *SKA2* [61, 62] genes, and neuroimaging measures of structure and function from the frontal cortex, hippocampus, and amygdala. Findings show that peripheral 5mC can index CNS structural

variability[55-62] associated with psychiatric illness development, and that locus-specific peripheral 5mC can mediate ASE-associated CNS structure variability[62].

To date, however, limited work has investigated the relationships among ASEs, peripheral 5mC, and CNS endophenotypes of psychiatric illness at a genome-scale. To this end, the current exploratory study applied genome-scale approaches in an all-female, African American sample from the Grady Trauma Project (GTP) to assess whether blood-derived 5mC measurements might index CNS endophenotypes of stress-related psychiatric illness. We focus specifically on the GTP because African American women may be subject to elevated risk of stress-related psychiatric illness development, but the mechanisms underlying that elevated risk are still unclear. In this study, we were specifically interested whether clusters of peripheral 5mC measurements statistically mediate the relation between ASEs and fronto-limbic grey matter volume (GMV), SA, and CT measures. Based on previous work, we hypothesized that identified 5mC modules would be enriched with 5mC probes falling in genes with HPA-axis[44, 45], immune system[46, 47], and CNS-relevant [48-50] gene ontology (GO) functions.

Materials and Methods

Participants

The current research draws on 97 female, trauma-exposed participants. Participants were part of the GTP, a larger investigation of genetic and environmental factors that predict the response to stressful life events (SLEs) in a predominantly African American, low-income, urban population [15]. Research participants were approached in the waiting rooms of primary care clinics of a large, public hospital. After the subjects provided written informed consent, they participated in a verbal interview and gave a blood sample for genetic and epigenetic analyses. Participants in this cohort also had available demographic, psychosocial, and neuroimaging data. Exclusion criteria included intellectual disability or active psychosis. Participants provided written, informed consent for all parts of the study, and the Institutional Review Boards of Emory University and Grady Memorial Hospital approved the study procedures.

196 *Exposures of interest*

197 Income, education, adult trauma burden, and childhood trauma burden were considered exposures
198 of interest in current analyses. *Income:* Self-reported approximate household monthly income ("household
199 income") was measured as part of a demographic-focused inventory. Participants indicated total household
200 income within one of the following ranges: $0 to $499, $500 to $999, or greater than $1000 per month.
201 *Education:* Participants also reported educational attainment history ("education") and were binned into one
202 of the following categories: did not complete high school, completed high school or GED, or completed
203 more schooling than high school. *Traumatic events inventory:* Adult trauma burden was assessed via a
204 semi-structured interview using the Traumatic Events Inventory (TEI), a scale developed by the GTP
205 researchers during their prior work in the Grady hospital primary care population [63]. TEI responses
206 pertaining to childhood were excluded in favor of the Childhood Trauma Questionnaire (CTQ). In the current
207 study, the continuous TEI score was used ("TEI"); the higher the TEI score, the more traumatic life events
208 one encountered. *Childhood trauma questionnaire:* Childhood trauma burden was assessed using the self-
209 report 28 question CTQ [64]. This inventory consists of five subscales, including sexual abuse, physical
210 abuse, emotional abuse, as well as physical and emotional neglect. In the current study, the total CTQ
211 score was used ("CTQ total"). Information regarding previous usage of exposure of interest variables in
212 GTP studies can be found elsewhere [15, 42, 65-68].

213 *Neuroimaging* Structural MRI study procedures followed the same methods as previously described in the
214 GTP cohort [69-72]. Structural images were acquired on a Siemens 3.0-Tesla Magnetom Trio TIM whole-
215 body MR scanner (Siemens, Malvern, PA, USA) with a 12-channel head coil, and using a gradient-echo,
216 T1-weighted pulse sequence (176 slices, TR = 2600 ms, TE = 3.02 ms, 1 mm^3 voxel size). The T1 scan
217 was processed using FreeSurfer (available at http://surfer.nmr.mgh.harvard.edu), and a standardized
218 protocol (available at http://enigma.ini.usc.edu/ protocols/imaging-protocols/) was used to check the
219 quality of the segmentations before further analyses were performed. Hemisphere-specific frontal cortex
220 CT and SA measurements were taken along with amygdala and hippocampal gray matter volume to
221 assess brain morphometry of the fronto-limbic pathway. For the purpose of the current study, within each
222 brain region (hippocampus and amygdala), we took the mean volume of the two hemispheres (e.g.,

hemisphere-mean hippocampal volume, hemisphere-mean amygdala volume). CT and SA develop along discordant temporal trajectories[73], and are affected in different manners based on underlying genetic sequence[74]. Based on this rationale, we examined CT and SA measures of frontal cortex subregions, instead of gray matter volume. Frontal cortex subregions included in the current study map to Brodmann's areas 8, 9, 10, 11, 24, 25, 32, and 46[25], and include FP, medial OFC (mOFC), lateral OFC (lOFC), SFG, RMFG, rostral ACC (rACC), and caudal ACC (cACC). For frontal cortex SA and CT, we used an average of values taken across hemispheres (e.g., hemisphere-mean RMFG SA, hemisphere-mean RMFG CT).

Molecular

Whole-blood was collected in EDTA vacuum tubes prior to DNA extraction. Genomic DNA was extracted and purified using the AllPrep DNA/RNA Mini Kit (Qiagen, Valencia, CA) using manufacturer recommended methods. DNA was denatured and bisulfite converted (BSC) using the EZ DNA Methylation-GoldTM Kit (Zymo Research, Irvine, CA). After conversion, BSC DNA was applied to the Infinium MethylationEPIC BeadChip (Illumina; San Diego, California) (850k) using manufacturer recommended protocol to measure DNA 5mC at ~850,000 loci.

5mC pre-processing

Beta-values measured from the 850k platform were background corrected with GenomeStudio, quality controlled (QCed), and filtered according to previously published methods[75]. All quality control and pre-processing was performed in R version 3.6.1[76]. These steps removed low quality and potentially cross-hybridizing probes, quantile-normalized probe Beta-values, and removed technical and batch effects[77-80]. 5mC beta-values were variance stabilized and logit-transformed into M-values[81]. X- and Y-chromosome-mapped probes were removed, along with *rs*-mapped probes. The remaining ~827k probes were then subset to include only those with observed nominally significant Pearson correlation ($p < 0.05$) between blood and brain tissue from the ImageCpG data repository[82], which focused analysis onto loci with greater prospect for proxy or surrogate status with etiologically-relevant CNS tissue. Following QC and filtering steps, 92,208 probes remained.

Covariates

Age, leukocyte cell estimates, intra-cranial volume (ICV), multi-dimensional scaling (MDS) of genomic ancestry, an epigenetic proxy of smoking[83], and current employment/disability status were included in models as covariates, where pertinent. *Leukocyte cell estimates:* DNAm measurements were used to estimate the proportions of granulocytes, monocytes, B cells, natural killer cells, CD4T and CD8T cells within each sample. Calculations were done according to methodology described in Houseman et al[84]. Estimated proportions of monocytes, B cells, natural killer cells, CD4T and CD8T were included as covariates in multiple regression models, where pertinent. *Genomic ancestry:* To avoid potential inaccuracies/confounding effects of self-reported race/ethnicity, genetic ancestry was modeled using MDS measures extracted from participant genome-wide association study (GWAS) data using PLINK[85]. The first four MDS genetic ancestry measures were chosen to be used as covariates based on visual inspection of scree plots, in line with previous work[86]. *Smoking:* Cigarette smoking is known to exert significant effects across the methylome[87]. Using a method discussed in detail elsewhere[88], the current study corrected for the methylomic effects of smoking by calculating effect size estimates of the top twenty-six probes from a recent smoking epigenome-wide association study (EWAS) performed in participants with African American genomic ancestry[83]. *Employment and disability:* As applied previously in the GTP [66], employment/disability status was considered as: unemployed; unemployed receiving disability support; or employed, with or without disability support.

Probe clustering

To remove non-desired effects from probe M-values, we composed linear models in R using age, leukocyte cell esimates, genomic ancestry, and the smoking proxy as predictors of probe-wise 5mC M-values. For each probe, residual values ("residualized M-values") were extracted for clustering. Taking the 92,208 residualized M-values, the "WGCNA" package was then used in R to build a co-methylation network[89]. First, scale-free topology model fit was analyzed. As recommended, a soft-threshold value of ten was chosen based on the lowest power at which adjusted $R^2 > 0.90$. Adjacency and dissimilarity matrices were generated, and unsupervised hierarchical clustering was used to generate a clustered residual M-value network. Setting a minimum cluster size of ten generated 73 clusters of 5mC probes,

where each cluster was identified by a unique color. After clustering, we extracted the first principal component of each cluster, referred to from here on as a “module eigengene” (ME). Compared to EWAS-type analyses, which assess differential methylation on the level of individual 5mC loci, network-based methods, as used in the current research, utilize dimension-reduction techniques to create networks of related 5mC probe clusters. This reduces the burden of multiple hypothesis testing across hundreds of thousands of probes, while enabling investigation into the biological significance of clustered probes, and provides the potential for increased statistical power in circumstances with a small number of biological replicates[90].

Statistical analyses

To understand the relationships between variables used throughout the current analyses, we carried out Pearson correlations and mapped their correlation coefficients. We then conducted a set of multi-variate linear regression analyses, as shown in Figure 1. Figure 1 Arm A analyses included hemisphere-mean hippocampus and amygdala volumes as dependent variables (in separate models). Income, education, CTQ total, and TEI were included as independent variables of interest, whereas genomic ancestry, age, employment/disability and ICV were included as covariates. The same predictors and covariates were included, minus ICV, to predict frontal cortex subregions SA and CT measures. Overall CT and/or SA were not included as covariates based on prior work with this cohort[91]. Figure 1 Arm B analyses included 5mC MEs as dependent variables (in separate models). Income, education, CTQ total, and TEI were included as independent variables of interest, and employment/disability was included as a covariate. Covariates were limited in this stage of analysis due to the removal of confounding effects through residual extraction in prior pre-processing steps. Figure 1 Arm C analyses included individual fronto-limbic morphometry measures as dependent variables (in separate models). Individual 5mC MEs were included as independent variables of interest, whereas age, genomic ancestry, employment, and ICV (ICV was only included in hippocampus and amygdala models) were included as covariates. Within each phase of the analyses, including mediation analyses, continuous dependent and independent variables were standardized, resulting in standardized effect estimates. Nominal p-values were corrected for multiple hypothesis testing by controlling the false discovery rate (FDR=0.10) using the Benjamini Hochberg (BH)

procedure(85). Briefly, for each nominal p-value, a BH critical value was calculated where nominal p-value's assigned rank over the number of tests was multiplied by the accepted FDR. Nominal p-values less than this threshold were deemed BH-significant. Due to the exploratory nature of the current work, both nominal and BH-significant terms were considered for interpretation; and nominal p-values are presented within the results section of the current text.

Mediation analyses

MEs were tested for statistical mediating status between independent variables of interest (ASEs) and dependent variables (hemisphere-mean fronto-limbic brain morphometry) using the "mediation" package in R (Figure 1). Importantly, only fronto-limbic brain morphometry measures nominally associated with income, education, CTQ total or TEI (Figure 1, Arm A) were considered. Similarly, MEs tested for mediation included only those nominally associated with an exposure (Figure 1, Arm B) and a fronto-limbic brain morphometry measure (Figure 1, Arm C). For each ME, average indirect effect (IDE), direct effect (DE), and total effect estimates and confidence intervals were calculated as a result of 10,000 quasi-Bayesian Monte Carlo approximations, applied with the mediation package. Consistent with methodology employed in the field [92, 93], we considered an ME a full mediator if the DE=0 while the IDE and total effect $\neq 0$, or a partial mediator if the DE, IDE, and total effect (TE) $\neq 0$. Individual probes from full mediator modules were assessed for mediation status, in order to gain insight into potential locus-specific mediation effects.

Gene set enrichment analyses

To assess underlying methylomic network enrichment, all four ASEs of interest were included in linear models as either independent variables or covariates, where individual residualized probe M-values were included as dependent variables, while controlling for employment/disability status. Importantly, only exposures with a fully-mediating 5mC cluster were considered independent variables of interest. Other exposures which did not exhibit a fully-mediating 5mC cluster were considered as covariates. For probes/ASEs with nominally significant relationships ($p < 0.05$), we extracted probe p-values and probe names and used them as input to gene set enrichment analyses (GSEA) with the "methylGSA" package[94].

Importantly, ASE-associated probe p-values were only captured for ASEs in which a full mediator was previously observed, which limited analyses to CTQ only. GO sets of 25 to 1,000 genes were allowed, eliminating high-level GO-terms such as “biological process”, which facilitated testing of 5,478 gene sets. To produce a condensed summary of non-redundant GO-terms, the web-based tool “Revigo” was used[95].

Results

Study participants

Descriptive statistics for demographic and psychosocial measures in study participants are shown in Table 1. Thirty percent of the sample reported household income in the range of $0 to $499 per month, while 34% of the sample reported household income above $1000 per month. Fifteen percent of the sample reported not having finished high school, whereas 55% of the sample reported having more schooling than high school. Mean CTQ total value for participants was 40.5 (+/- 15.4), whereas mean TEI value for participants was 4.2 (+/- 2.3). Pearson correlations between variables used in the current study are shown in Figure 2.

ASEs predict fronto-limbic brain morphometry

At nominal significance, CTQ total was negatively associated with RMFG SA (β = - 0.231, SE = 0.111, t = - 2.079, p = 0.041), but was not associated with other outcomes of interest ($p > 0.05$). Relative to high educational attainment (completed more schooling than high school), low educational attainment (no high school certificate) was negatively associated with cACC SA (β = - 0.855, SE = 0.280, t = - 3.049, p = 0.003), and positively associated with FP CT (β = 0.684, SE = 0.302, t = 2.267, p = 0.026) and SFG CT (β = 0.553, SE = 0.256, t = 2.162, p = 0.034) at the nominal significance threshold, but no other brain morphometry outcomes of interest ($p > 0.05$). On the other hand, relative to high income ($1000+/month), low income ($0-$499/month) was nominally negatively associated with amygdala GMV (β = - 0.649, SE = 0.283, t = - 2.299, p = 0.024), but no other neuroimaging outcome of interest ($p > 0.05$). TEI was not associated with any neuroimaging measures ($p > 0.05$). Nominally significant model outcomes can be found in Table 2. In controlling for 64 total tests at FDR = 0.10, no outcomes were BH-significant. Brain morphometry outcomes nominally associated with ASEs were carried into downstream analyses.

ASEs predict 5mC ME

CTQ total was nominally associated with seven MEs, the strongest of which were Darkolivegreen (Darkolivegreen β = 0.354, SE = 0.110, t = 3.214, p = 0.002) and Steelblue (Steelblue β = - 0.306, SE = 0.111, t = - 2.748, p = 0.007). Compared to high educational attainment, low educational attainment was positively associated with one ME (Coral1 β = 0.750, SE = 0.286, t = 2.618, p = 0.010), and negatively associated with one ME (Lightcoral β = - 0.615, SE = 0.296, t = - 2.079, p = 0.040) at nominal levels. Relative to high income ($1000+/month), low income ($0-$499/month) was positively associated with three MEs (Antiquewhite4 β = 0.770, SE = 0.277, t = 2.781, p = 0.007; Indianred4 β = 0.717, SE = 0.276, t = 2.602, p = 0.011; Orange β = 0.571, SE = 0.274, t = 2.084, p = 0.040) at nominal levels. Because TEI was not associated with any fronto-limbic brain morphometric measures (Figure 1, Arm A), we do not report any results for this exposure. Results from all Arm B analyses can be found in Supplementary Table 1. In controlling for 73 tests at FDR = 0.10, no outcomes were BH-significant. 5mC MEs nominally associated with ASEs were carried into downstream analyses.

5mC MEs predict fronto-limbic brain morphometry

Four out of seven CTQ-associated MEs showed a nominally significant relationship with hemisphere-mean RMFG SA (Maroon, White, Tan, Yellow). The three strongest relationships were the Maroon ME (β = - 0.451, SE = 0.091, t = - 4.966, p = $3x10^{-6}$) (Figure 3a), White ME (β = - 0.392, SE = 0.093, t = - 4.231, p = $6x10^{-5}$) (Figure 3b), and Tan ME (β = 0.233, SE = 0.100, t = 2.322, p = 0.023) (Figure 3c). Two low educational attainment-associated MEs were tested independently for associations with hemisphere-mean cACC SA, frontal pole CT, and SFG CT. Of these, the Lightcoral ME was nominally associated with cACC SA (β = 0.215, SE = 0.099, t = 2.182, p = 0.032) (Figure 3d). Finally, of the three low income-associated MEs, none showed a nominally significant relationship with hemisphere-mean amygdala volume (Supplementary Table 2). In controlling for 16 tests at FDR = 0.10, the Maroon and White ME relationships with hemisphere-mean RMFG SA were BH-significant. 5mC MEs nominally associated with fronto-limbic brain morphometry measures were carried into downstream analyses.

ME mediation

Four CTQ-associated MEs that also showed a nominally significant relationship with hemisphere-mean RMFG SA were tested for their mediating status between CTQ total and hemisphere-mean RMFG SA (Maroon, White, Tan, Yellow). Both the Maroon ME (TE β = -0.983, p = 0.047; IDE β = -0.466, p = 0.008; DE β = -0.517, p = 0.277) and the White ME (TE β = -1.014, p = 0.034; IDE β = -0.348, p = 0.032; DE β = -0.667, p = 0.164) were full mediators of this relationship. TE results show that RMFG SA was an estimated ~589 mm^2 lower at the highest levels of CTQ exposure compared to the lowest levels of CTQ exposure. Independently, the Maroon ME accounted for 275 mm^2 (47%) of that effect, whereas the White ME accounted for 204 mm^2 (34%). Neither the Tan nor Yellow MEs were partial or full mediators of the relationship between CTQ and hemisphere-mean RMFG SA (TE $p < 0.05$; IDE $p > 0.05$; DE $p > 0.05$), although the direction of TEs in these analyses closely mirrored those in the Maroon and White ME mediation analyses. The Lightcoral ME, which we previously observed to be associated with low education attainment and cACC SA, was neither a partial nor full mediator of the relationship between low education attainment and hemisphere-mean cACC SA (TE β = -0.844, p = 0.003; IDE β = -0.107, p = 0.100; DE β = -0.737, p = 0.010). However, the DE indicates that low educational attainment status accounted for cACC SA that is 84 mm^2 smaller than high educational attainment status. In controlling for ten tests of the IDE and DE p-values for the five relationships above at FDR = 0.10, all nominally significant ME IDEs were BH-significant and all DEs remained non-significant (Table 3). Follow-up mediation analyses were then performed on individual probes from the Maroon and White modules.

Probe-wise mediation: Maroon module

Six out of the 11 Maroon ME probes were full mediators of the relationship between CTQ total and RMFG SA (Table 4). The top three strongest mediators based on IDE β coefficients were: cg21622733 (TE β = -0.983, p = 0.044; IDE β = -0.512, p = 0.003; DE β = -0.471, p = 0.320), cg19805668 (TE β = -1.003, p = 0.042; IDE β = -0.411, p = 0.009; DE β = -0.592, p = 0.217), and cg03710029 (TE β = -0.990, p = 0.048; IDE β = -0.321, p = 0.019; DE β = -0.670, p = 0.182). Respectively, these probes mapped to the long intergenic non-coding (LINC) RNA gene *LINC01531*, the placental growth factor gene *PGF*, and the solute carrier family 38 member 10 gene *SLC38A10*. The other three full mediating probes mapped to myosin

heavy chain 14 (*MYH14*), DNA methyltransferase 3 alpha (*DNMT3A*), and neuralized E3 ubiquitin protein ligase 4 (*NEURL4).* In controlling for 22 tests of Maroon probe IDE and DE p-values, only two nominally significant probes were also BH-significant (cg21622733: *LINC01531* and cg19805668: *PGF*). Comprehensive probe-wise mediation results are found in Supplementary Table 3.

In all, probes from the Maroon module map to eight known protein coding genes (*MYH14, HGSNAT, SFTPA1, PGF, NEURL4, DNMT3A, SLC38A10,* and *PEBP4*) and two non-coding RNAs (*LINC01531 and MIR3659HG*). GO-terms associated with these loci include: *MYH14* (neuronal action potential GO:0019228, actomyosin structure organization GO:0031032), *HGSNAT* (lysosomal transport GO:0007041, neutrophil degranulation GO:0043312), *SFTPA1* (toll-like receptor signaling pathway GO:0002224), *PGF* (chemoattractant activity GO:0042056, vascular endothelial growth factor receptor binding GO:0005172), *NEURL4* (ubiquitin protein ligase activity GO:0061630), *DNMT3A* (DNA (cytosine-5-methyltransferase activity GO:0003886), *SLC38A10* (amino acid transmembrane transporter activity GO:0015171), and *PEBP4* (protein binding GO:0005515), among others.

Probe-wise mediation: White module

Three out of 19 White ME probes were full mediators of the relationship between CTQ total and RMFG SA (Table 4): cg01544227 (TE β = -0.994, p = 0.044; IDE β = -0.305, p = 0.036; DE β = -0.689, p = 0.175), cg00686169 (TE β = -1.017, p = 0.037; IDE β = -0.277, p = 0.043; DE β = -0.740, p = 0.126), and cg08002107 (TE β = -1.006, p = 0.040; IDE β = -0.268, p = 0.047; DE β = -0.738, p = 0.122). These three probes mapped to *AC092745.5*, *FAM90A24P*, and *USP17L7* loci, respectively. In controlling for 38 tests of White probe IDE and DE p-values, no nominally significant probes were BH-significant. Comprehensive probe-wise mediation results are found in Supplementary Table 3.

In all, only one probe from the White module maps to a known protein coding gene, *USP17L7*, which is associated with the thiol-dependent de-ubiquitinase GO term (GO:0004843*).* One other probe maps to a LINC RNA, *FAM66D*. The remaining probes map to a pseudogene family, named family with sequence similarity 90. Members include: *FAM90A10*, *FAM90A11P*, *FAM90A20*, *FAM90A24P*, *FAM90A25P*, *FAM90A5*, *FAM90A6P*, and *FAM90A7*. The only GO term associated with these pseudogenes is nucleic acid binding (GO:0003676).

Gene set enrichment analysis

CTQ total was included as the independent variable of interest in linear models with probe residualized M-values as dependent variables. Income, education, and TEI were included and considered as covariates, as no 5mC clusters mediated the relationships between our exposures and outcomes of interest. We used the resultant 6,335 nominally significant p-values and probe names as GSEA input, facilitating the testing of 5,478 GO-terms. After Revigo redundancy reduction, 30 BH-significant GO-terms remained for interpretation. These included immune-related GO-terms: macrophage migration (GO:1905517, $p = 9x10^{-8}$, rank = 10), T cell receptor complex (GO:0042101, $p = 6x10^{-6}$, rank = 13), and chemokine-mediated signaling pathway (GO:0070098, $p = 7x10^{-4}$, rank = 28), among four others. Two CNS-related GO-terms were present: negative regulation of smoothened signaling pathway (GO:0045879, $p = 2x10^{-6}$, rank = 12), and glutamine family amino acid biosynthetic process (GO:0009084, $p = 1x10^{-4}$, rank = 19), along with one HPA-axis related term: thyroid hormone metabolic process (GO:0042403, $p = 2x10^{-15}$, rank = 5). Additionally, numerous signal transduction and membrane transport GO-terms were present: positive regulation of phospholipase activity (GO:0010518, $p = 5x10^{-25}$, rank = 1), intrinsic component of peroxisomal membrane (GO:0031231, $p = 7x10^{-18}$, rank = 2), and RNA polymerase II carboxy-terminal domain kinase activity (GO:0008353, $p = 8x10^{-15}$, rank = 6), among others (Supplementary Table 4).

Discussion

Here we applied genome-scale approaches to a sample of African American women from a low income, highly trauma exposed environment, representing an understudied population, where our main goal was to assess whether blood-derived 5mC cluster MEs might index CNS endophenotypes of stress-related psychiatric illness. Our study findings indicate that high childhood trauma burden, low educational attainment, and low income are each associated with CNS endophenotypes of stress-related psychiatric illness, and that a subset of blood-derived 5mC MEs statistically mediate the relationship between childhood trauma burden and RMFG SA. We further found that the individual probes from mediating 5mC MEs fell in genes with CNS-relevant and immune system GO-functions. Finally, we found that the underlying childhood trauma burden-associated methylomic network was enriched with HPA-axis, immune, and CNS-related

gene sets, in addition to signal transduction and membrane transport functions. Overall, we posit that the peripheral epigenetic signatures mediating our relationships of interest are consistent with previously observed patterns in which stress-related psychiatric illness is accompanied by profiles of peripheral inflammation[31, 96-98].

In the current study, childhood trauma burden was negatively associated with hemisphere-mean RMFG SA, which mirrors findings from cohorts enriched for stress, trauma, and psychiatric illness[99, 100]. We also observed higher CT of both the FP and SFG in participants with low educational attainment, as well as higher cACC SA. Although studies on FP CT and ASEs (besides trauma) are somewhat limited, our findings support past research investigating whether high CT is representative of a predisposition to psychiatric illness development, or whether high CT emerges after psychiatric illness onset. Specifically, prior longitudinal work showed higher cortical thickness in participants at high risk of mood disorder compared to healthy controls at baseline; the high-risk participants who went on to develop MDD then showed increased FP CT over the two-year time period following their diagnosis[101]. This research implies that high FP CT could represent both a predisposition to MDD development risk, and a post-onset emergent phenotype of MDD.

Our study also showed that low household income was negatively associated with hemisphere-mean amygdala GMV. This finding aligns with research in children/adolescents showing that low familial income-to-needs ratio is associated with decreased amygdala GMV [92], and with studies in adults showing that past year financial hardship is associated with decreased amygdala GMV [102]. However, the relationships between socioeconomic status-related measures and amygdala GMV are well-studied, and variable conclusions between studies are common[103]. Hemisphere-mean hippocampal volume was not associated with any ASE; as in the case of amygdala GMV, study conclusions are mixed[103].

In all, four blood-derived MEs were tested for mediating status between childhood trauma burden and RMFG SA. Both the Maroon and the White ME fully mediated the relationship and accounted for significant proportions of variability (47% and 35% respectively). The Maroon module is composed of 11 probes, six of which are also full mediators of the aforementioned relationship. The six probes fully mediating the childhood trauma burden and RMFG SA relationship are located in the *MYH14, PGF, NEURL4, DNMT3A, SLC38A10,* and *LINC01531.* GO-terms associated with these loci include: *MYH14*

(neuronal action potential GO:0019228, actomyosin structure organization GO:0031032), *PGF* (chemoattractant activity GO:0042056, vascular endothelial growth factor receptor binding GO:0005172), *NEURL4* (ubiquitin protein ligase activity GO:0061630), *DNMT3A* (DNA (cytosine-5-methyltransferase activity GO:0003886), and *SLC38A10* (amino acid transmembrane transporter activity GO:0015171). Of particular interest is the probe falling in the *DNMT3A* gene. Past longitudinal study in a predominantly female African American sample showed differential blood *DNMT3A* 5mC in response to traumatic event exposure[104], and emerging work focused specifically on African ancestry individuals has identified a genome-wide significant association in *DNMT3A* in relation to MDD[105]. What is more, in a rodent model of fear conditioning, *Dnmt3a* mRNA expression is altered in forebrain neurons, leading to differential DNA 5mC of synaptic plasticity and memory formation genes[106]. *Dnmt3A* mRNA expression in rodent nucleus accumbens is also altered in response to chronic restraint stress, and targeted inhibition of *Dnmt3A* 5mC potentiates anti-depressant-like effects[107]. Based on the current and prior findings, it appears that the *DNMT3A* gene in humans is a potential locus of stress- or trauma-related biological embedding, and that measurements of *DNMT3A* 5mC taken from peripheral tissues could be indexing fronto-limbic variability associated with these exposures. Overall, our findings in the Maroon module imply that immune signaling, cellular proliferation, neuronal development, and epigenetic regulatory pathways could be potential substrates for the biological embedding of childhood trauma.

The second fully mediating ME was the White module comprised of 19 probes, three of which were full mediators of the relation between CTQ total and RMFG SA. Thirteen probes from this module are mapped to the “Family with sequence similarity 90” superfamily of pseudogenes, and all but two probes exist in a one megabase stretch of chromosome eight. The three full mediator probes (cg00686169, cg01544227, and cg08002107) fall in the *FAM90A24P, LINC00937, and FAM66D* loci, respectively. Little is known of the *FAM90A24P* locus, but the *LINC00937* locus encodes a LINC RNA species that is strongly associated with cutaneous melanoma prognosis[108], as well as endocervical cancer progression[109], suggesting that it plays a role in cellular proliferation. On the other hand, the *FAM66D* locus encodes a LINC RNA species whose expression is significantly upregulated in both Crohn’s disease (CD) and ulcerative colitis (UC), the two most common types of inflammatory bowel disease (IBD)[110]. Efforts made towards elucidating the function of the broader chromosome eight locus highlight its structurally dynamic

nature, in addition to its harboring of the defensin genes, the protein products of which play significant roles in the innate immune response, as well as antitumor response[111]. Defensin proteins are also recognized as key contributors to innate immune defense against UC, CD, and IBD in general[112].

Taken together, results suggest that probes mediating the childhood trauma burden and RMFG SA relationship interact with endothelial growth and innate immune response regulatory pathways. This notion is supported by repeated observation of increased blood-based inflammation profiles, as measured in adults that had previously experienced childhood trauma exposure [113-115]. More CNS-focused research has also shown significant dysregulation of stress-response and inflammation-related mRNA/protein levels in post-mortem frontal cortex of patients with neurodevelopmental[116] and psychiatric illnesses[117, 118]. What is more, decreased CT of medial pre-frontal cortex is observed in MDD patients, a relationship that was partially mediated by inflammatory factors known to influence neuroplasticity[119]. However, the relevant studies informing our current results are sparse, and could be considered underpowered. Thus, while suggestive, more work remains to be done in order to draw robust inferences regarding the relationship between peripheral inflammation and neural endophenotypes of stress-related psychiatric illness.

In our GSEA of childhood trauma burden -associated probes, the top enriched term was “positive regulation of phospholipase activity”, meaning that multiple probes fall in genes that increase the frequency, rate, or extent of phospholipase activity. Of close relation is the 11th ranked GO-term, “inositol phosphate phosphatase activity”. Together, these terms represent one of the major mechanisms of neuronal and hormonal signal transduction in mammals, the activation of phospholipase C (PLC) and subsequent activation of inositol signaling pathways[120]. In brief, extracellular stimuli receptor binding activates PLC. PLC then functions to convert phosphatidylinositol-4-5 bisphosphate (P45P2) into inositol-1-4-5 trisphosphate (I145P3). From this, the kinase-activating secondary messenger diacylglycerol (DAG) is activated[120]. There are many isoforms of the PLC enzyme family, but PLC-δ1 is strongly implicated in regulating cell-motility and cytoskeletal organization[121], and in inhibiting inflammatory immune responses[122]. Quantities of this PLC isoform, PLC-δ1, are highly correlated with nuclear levels of P45P2[123]; interestingly, P45P2 regulates transcription through binding interaction with the RNA polymerase II C-terminal tail[124]. The aforementioned processes are specifically represented within our

GSEA results (Supplementary Table 4): RNA polymerase II carboxy-terminal domain kinase activity, regulation of mitotic spindle organization, and numerous immune signaling and motility terms. Given childhood trauma burden is the ASE implicated most strongly in our results, it stands to reason that in this sample of African American women, peripheral inflammatory signals could be heightened in those with high childhood trauma burden, and phospholipase activity may be upregulated in an attempt to restore homeostatic balance.

Overall, we posit that the blood-based epigenetic signatures mediating our relationships of interest are potentially explained by ASE-associated peripheral inflammation. In response to perceived stress or trauma, fronto-limbic brain regions associated with cognitive function, emotional reactivity, and memory are activated, signaling to the HPA-axis' neural hub, and eventually potentiating glucocorticoid (GC) release. Critical to immunological, metabolic, cardiac, and homeostatic functions, GCs act mechanistically in and around the CNS and peripheral nervous system, including serving as a long-range negative feedback mechanism to inhibit further HPA-axis activity. Additionally, the ligands and receptors of cytokines and neurotransmitters are shared throughout the CNS, HPA-axis, and immune systems[125, 126]. Chronic stress signaling can result in neural growth, inflammation, metabolism, and stress-related pathway disruption through molecular and epigenetic mechanisms[40], which are consistent with 5mC-derived patterns observed in peripheral tissue in the current report.

The foremost strength of the current research is the inclusion of multi-modal data types (epigenetic/neuroimaging) to characterize the biological embedding of ASEs. Furthermore, the dimension reduction techniques used in the current work, clustering and principal component extraction, were valuable in reducing the burden of multiple hypothesis testing and in describing potentially related networks of 5mC loci. It also focused the analysis onto loci with greater prospect for proxy or surrogate status with etiologically-relevant CNS tissue. The composition of the sample is also a strength of the current work, as it reflects an understudied population at elevated risk for PTSD and for persistence of stress-related psychiatric illness[127]. However, because of the homogenous nature of the sample, we are unable to make confident conclusions about ancestry-specific or sex-specific effects. Limitations of the current study include relatively small sample size and the inability to infer causality from cross-sectional samples. In addition, the current research used peripheral tissue in lieu of etiological CNS tissue for obvious technical reasons.

Functional MRI measures such as neurotransmitter specific PET imaging could also provide deeper endophenotypic insights. Future studies on this topic should capture longitudinal data from a larger sample and could investigate genetic factors or tissues of etiological interest.

The current study showed that exposure to high childhood trauma burden, low educational attainment, and low income are each associated with neuroimaging endophenotypes of psychiatric illness, and that the relationship between childhood trauma and RFMG SA in particular is mediated by a subset of blood-derived 5mC measurements. In addition, we found that the mediating 5mC MEs were enriched with probes falling in genomic regulatory regions, and in genes with CNS-relevant and immune system GO-functions. Finally, we found that the underlying childhood trauma burden-associated methylomic network was enriched with HPA-axis, immune, and CNS-related gene sets. Together, these results highlight a feasible epigenetic mechanism through which ASEs become embedded in human physiological systems, and through which they contribute to the development of stress-related psychiatric illness. Although these concepts are broadly applicable across race, ethnicity, and biological sex, the current results highlight mechanisms of biological embedding that may be specific to African American women. These epigenetic signatures could be taken as peripheral biomarkers of perturbed underlying neurobiology associated with ASEs, and could further research efforts into etiological tissues of interest such as endocrine, immune, and CNS cell types. These findings could also serve to potentiate increased investigation of understudied populations at significant risk for onset or persistence of certain stress-related psychiatric illnesses.

Acknowledgements

This work was supported by the National Institutes of Mental Health (MH096764, MH071537, MH098212, MH111671, MH101380 and 2R01MH108826) and the National Institute of Minority Health and Health Disparities (2R01MD011728). Support was also received from Emory and Grady Memorial Hospital General Clinical Research Center, NIH National Centers for Research Resources (M01RR00039) and Howard Hughes Medical Institute.

Conflict of interest

The authors report no conflicts of interest.

Data Availability Statement

DNA methylation data analyzed in this paper are available at https://www.ncbi.nlm.nih.gov/geo/ (dataset GSE132203). Individual-level neuroimaging data will be made available to researchers following an approved analysis proposal through the GTP. For additional information on access to these data, including PI contact information for the GTP, please contact the corresponding author.

Figure Legends

Figure 1. Conceptual model testing individual module eigengenes (MEs) as mediators of the hypothesized associations between adverse social exposures (ASEs) and variability in fronto-limbic brain morphometries. Arm A. Analyses included hemisphere-mean hippocampus and amygdala volumes as dependent variables (in separate models). Income, education, CTQ total, and TEI were included as independent variables of interest, whereas genomic ancestry, age, employment/disability and ICV were included as covariates. The same predictors and covariates were included, minus ICV, to predict frontal cortex subregions SA and CT measures. Arm B. Analyses included 5mC MEs as dependent variables (in separate models). Income, education, CTQ total, and TEI were included as independent variables of interest, and employment/disability was included as a covariate. Arm C. Analyses included individual fronto-limbic morphometry measures as dependent variables (in separate models). Individual 5mC MEs were included as independent variables of interest, whereas age, genomic ancestry, employment, and ICV (ICV was only included in hippocampus and amygdala models) were included as covariates.

Figure 2. Pearson's correlation heatmap of variables used throughout the current study. Age is negatively associated with multiple frontal cortex cortical thickness (CT) measures (Pearson's correlation r_{range} = -0.15 to -0.47, p_{range} = 0.092 to $6x10^{-7}$). Within frontal cortex CT measures, multiple subregions show positive correlations with one another (Pearson's correlation r_{range} = 0.32 to 0.84, p_{range} = 0.004 to < $2x10^{-16}$). The same phenomenon is observed within frontal cortex surface area (SA) measures (Pearson's correlation r_{range} = 0.16 to 0.77, p_{range} = 0.210 to <$2x10^{-16}$). Overall CT is positively correlated with each of the frontal cortex CT measures (Pearson's correlation r_{range} = 0.43 to 0.86, p_{range} = $1x10^{-7}$ to <$2x10^{-16}$), and overall SA is positively correlated with each of the frontal cortex SA measures (Pearson's correlation r_{range} = 0.37 to 0.88, p_{range} = $5x10^{-4}$ to < $2x10^{-16}$).

Figure 3. CTQ total is negatively associated with rostral middle frontal gyrus (RMFG) surface area (SA). Low educational attainment status is associated with low caudal anterior cingulate cortex (cACC) SA. Out of seven CTQ-associated module eigengenes (MEs), the three strongest relationships with hemisphere-mean RMFG SA were the Maroon (A), White (B), and Tan (C) MEs. Out of two low education attainment-associated MEs, the strongest relationship with hemisphere-mean cACC SA was the Lightcoral ME (D). As shown, neuroimaging measures are adjusted by age, ME value, genomic ancestry, employment/disability status, and an adverse social exposure (ASE). Dependent and independent variables were scaled. A. CTQ total was positively associated with the Maroon ME (β = 0.289, SE = 0.109, t = 2.639, p = $9.8x10^{-3}$). In turn, the Maroon ME was negatively associated with RMFG SA (β = - 0.451, SE = 0.091, t = - 4.966, p = $3x10^{-6}$). B. CTQ total was negatively associated with the Tan ME (β = - 0.248, SE = 0.112, t = - 2.220, p = 0.029). The Tan ME was, in turn, positively associated with RMFG SA (β = 0.233, SE = 0.100, t = 2.322, p = 0.023). C. CTQ total was positively associated with the White ME (β = 0.236, SE = 0.110, t = 2.151, p = 0.034). In turn, the White ME was negatively associated with RMFG SA (β = - 0.392, SE = 0.093, t = - 4.231, p = $6x10^{-5}$). D. Low educational attainment (no high school certificate) was associated with the Lightcoral ME (β = - 0.615, SE = 0.296, t = - 2.079, p = 0.040). The Lightcoral ME, in turn, was positively associated with cACC SA (β = 0.215, SE = 0.099, t = 2.182, p = 0.032).

References

1. Semega J, Kollar M, Creamer J, and Mohanty A. *Income and poverty in the United States: 2018* 2019; Available from: https://www. census. gov/library/publications/2019/demo/p60-266. html. 2019.
2. Martin A, Markhvida M, Hallegatte S, and Walsh B. Socio-Economic Impacts of COVID-19 on Household Consumption and Poverty. *Economics of Disasters and Climate Change* 4, 453-479 (2020).
3. Tyler JH and Lofstrom M. Finishing High School: Alternative Pathways and Dropout Recovery. *The Future of Children* 19, 77-103 (2009).
4. Gilbert R, Widom CS, Browne K, Fergusson D, Webb E, and Janson S. Burden and consequences of child maltreatment in high-income countries. *The Lancet* 373, 68-81 (2009).
5. Roberts AL, Gilman SE, Breslau J, Breslau N, and Koenen KC. Race/ethnic differences in exposure to traumatic events, development of post-traumatic stress disorder, and treatment-seeking for post-traumatic stress disorder in the United States. *Psychological Medicine* 41, 71-83 (2011).
6. Kessler RC. Posttraumatic Stress Disorder in the National Comorbidity Survey. *Archives of General Psychiatry* 52, 1048 (1995).
7. Breslau N. The Epidemiology of Trauma, PTSD, and Other Posttrauma Disorders. *Trauma, Violence, & Abuse* 10, 198-210 (2009).
8. Kilpatrick DG, Resnick HS, Milanak ME, Miller MW, Keyes KM, and Friedman MJ. National Estimates of Exposure to Traumatic Events and PTSD Prevalence Using *DSM-IV* and *DSM-5* Criteria: *DSM-5* PTSD Prevalence. *Journal of Traumatic Stress* 26, 537-547 (2013).
9. Wadsworth ME, Raviv T, Santiago CD, and Etter EM. Testing the Adaptation to Poverty-Related Stress Model: Predicting Psychopathology Symptoms in Families Facing Economic Hardship. *Journal of Clinical Child & Adolescent Psychology* 40, 646-657 (2011).
10. Organization WH. Cross-national comparisons of the prevalences and correlates of mental disorders. WHO International Consortium in Psychiatric Epidemiology. *Bull World Health Organ* 78, 413-26 (2000).
11. Chevalier A and Feinstein L. Sheepskin or Prozac: The Causal Effect of Education on Mental Health. *SSRN Electronic Journal*, (2006).
12. Humphreys KL, LeMoult J, Wear JG, Piersiak HA, Lee A, and Gotlib IH. Child maltreatment and depression: A meta-analysis of studies using the Childhood Trauma Questionnaire. *Child Abuse & Neglect* 102, 104361 (2020).
13. Li M, D'Arcy C, and Meng X. Maltreatment in childhood substantially increases the risk of adult depression and anxiety in prospective cohort studies: systematic review, meta-analysis, and proportional attributable fractions. *Psychological Medicine* 46, 717-730 (2016).
14. McLaughlin KA, Alvarez K, Fillbrunn M, et al. Racial/ethnic variation in trauma-related psychopathology in the United States: a population-based study. *Psychological Medicine* 49, 2215-2226 (2019).
15. Gillespie CF, Bradley B, Mercer K, et al. Trauma exposure and stress-related disorders in inner city primary care patients. *General Hospital Psychiatry* 31, 505-514 (2009).
16. Holbrook TL, Hoyt DB, Stein MB, and Sieber WJ. Gender Differences in Long-Term Posttraumatic Stress Disorder Outcomes after Major Trauma: Women Are At Higher Risk of Adverse Outcomes than Men:. *The Journal of Trauma: Injury, Infection, and Critical Care* 53, 882-888 (2002).
17. Seedat S, Scott KM, Angermeyer MC, et al. Cross-National Associations Between Gender and Mental Disorders in the World Health Organization World Mental Health Surveys. *Archives of General Psychiatry* 66, 785 (2009).
18. Golub Y, Kaltwasser SF, Mauch CP, et al. Reduced hippocampus volume in the mouse model of Posttraumatic Stress Disorder. *Journal of Psychiatric Research* 45, 650-659 (2011).
19. Rosenkranz JA, Venheim ER, and Padival M. Chronic Stress Causes Amygdala Hyperexcitability in Rodents. *Biological Psychiatry* 67, 1128-1136 (2010).
20. Pagliaccio D, Luby JL, Bogdan R, et al. Stress-System Genes and Life Stress Predict Cortisol Levels and Amygdala and Hippocampal Volumes in Children. *Neuropsychopharmacology* 39, 1245-1253 (2014).
21. Hanson JL, Nacewicz BM, Sutterer MJ, et al. Behavioral Problems After Early Life Stress: Contributions of the Hippocampus and Amygdala. *Biological Psychiatry* 77, 314-323 (2015).

22. Swartz Johnna R, Knodt Annchen R, Radtke Spenser R, and Hariri Ahmad R. A Neural Biomarker of Psychological Vulnerability to Future Life Stress. *Neuron* 85, 505-511 (2015).
23. Teicher MH, Samson JA, Anderson CM, and Ohashi K. The effects of childhood maltreatment on brain structure, function and connectivity. *Nature Reviews Neuroscience* 17, 652-666 (2016).
24. Cassiers LLM, Sabbe BGC, Schmaal L, Veltman DJ, Penninx BWJH, and Van Den Eede F. Structural and Functional Brain Abnormalities Associated With Exposure to Different Childhood Trauma Subtypes: A Systematic Review of Neuroimaging Findings. *Frontiers in Psychiatry* 9, 329 (2018).
25. Kovner R, Oler JA, and Kalin NH. Cortico-Limbic Interactions Mediate Adaptive and Maladaptive Responses Relevant to Psychopathology. *American Journal of Psychiatry* 176, 987-999 (2019).
26. Gilbert SJ, Spengler S, Simons JS, et al. Functional Specialization within Rostral Prefrontal Cortex (Area 10): A Meta-analysis. *Journal of Cognitive Neuroscience* 18, 932-948 (2006).
27. Tsujimoto S, Genovesio A, and Wise SP. Frontal pole cortex: encoding ends at the end of the endbrain. *Trends in Cognitive Sciences* 15, 169-176 (2011).
28. Stevens FL, Hurley RA, and Taber KH. Anterior Cingulate Cortex: Unique Role in Cognition and Emotion. *The Journal of Neuropsychiatry and Clinical Neurosciences* 23, 121-125 (2011).
29. Bechara A. Emotion, Decision Making and the Orbitofrontal Cortex. *Cerebral Cortex* 10, 295-307 (2000).
30. Walter KH, Palmieri PA, and Gunstad J. More than symptom reduction: Changes in executive function over the course of PTSD treatment. *Journal of Traumatic Stress*, n/a-n/a (2010).
31. Misiak B, Beszłej JA, Kotowicz K, et al. Cytokine alterations and cognitive impairment in major depressive disorder: From putative mechanisms to novel treatment targets. *Progress in Neuro-Psychopharmacology and Biological Psychiatry* 80, 177-188 (2018).
32. Marganska A, Gallagher M, and Miranda R. Adult attachment, emotion dysregulation, and symptoms of depression and generalized anxiety disorder. *American Journal of Orthopsychiatry* 83, 131-141 (2013).
33. Green MF. Cognitive Impairment and Functional Outcome in Schizophrenia and Bipolar Disorder. *The Journal of Clinical Psychiatry* 67, e12 (2006).
34. Glahn DC, Thompson PM, and Blangero J. Neuroimaging endophenotypes: Strategies for finding genes influencing brain structure and function. *Human Brain Mapping* 28, 488-501 (2007).
35. Hasler G and Northoff G. Discovering imaging endophenotypes for major depression. *Molecular Psychiatry* 16, 604-619 (2011).
36. Matsubara T, Matsuo K, Harada K, et al. Distinct and Shared Endophenotypes of Neural Substrates in Bipolar and Major Depressive Disorders. *PLOS ONE* 11, e0168493 (2016).
37. Doom JR and Gunnar MR. Stress physiology and developmental psychopathology: Past, present, and future. *Development and Psychopathology* 25, 1359-1373 (2013).
38. O'Connor TG, Moynihan JA, and Caserta MT. Annual Research Review: The neuroinflammation hypothesis for stress and psychopathology in children - developmental psychoneuroimmunology. *Journal of Child Psychology and Psychiatry* 55, 615-631 (2014).
39. Dirven BCJ, Homberg JR, Kozicz T, and Henckens MJAG. Epigenetic programming of the neuroendocrine stress response by adult life stress. *Journal of Molecular Endocrinology* 59, R11-R31 (2017).
40. Jensen SKG, Berens AE, and Nelson CA. Effects of poverty on interacting biological systems underlying child development. *The Lancet Child & Adolescent Health* 1, 225-239 (2017).
41. Clayton DF, Anreiter I, Aristizabal M, Frankland PW, Binder EB, and Citri A. The role of the genome in experience-dependent plasticity: Extending the analogy of the genomic action potential. *Proceedings of the National Academy of Sciences* 117, 23252-23260 (2020).
42. Klengel T, Mehta D, Anacker C, et al. Allele-specific FKBP5 DNA demethylation mediates gene–childhood trauma interactions. *Nature Neuroscience* 16, 33-41 (2013).
43. Weaver ICG, *Integrating Early Life Experience, Gene Expression, Brain Development, and Emergent Phenotypes*, in *Advances in Genetics*. 2014, Elsevier. p. 277-307.
44. Perroud N, Paoloni-Giacobino A, Prada P, et al. Increased methylation of glucocorticoid receptor gene (NR3C1) in adults with a history of childhood maltreatment: a link with the severity and type of trauma. *Translational Psychiatry* 1, e59-e59 (2011).

45. Tyrka AR, Price LH, Marsit C, Walters OC, and Carpenter LL. Childhood Adversity and Epigenetic Modulation of the Leukocyte Glucocorticoid Receptor: Preliminary Findings in Healthy Adults. *PLoS ONE* 7, e30148 (2012).
46. Uddin M, Aiello AE, Wildman DE, et al. Epigenetic and immune function profiles associated with posttraumatic stress disorder. *Proceedings of the National Academy of Sciences* 107, 9470-9475 (2010).
47. Smith AK, Conneely KN, Kilaru V, et al. Differential immune system DNA methylation and cytokine regulation in post-traumatic stress disorder. *American Journal of Medical Genetics Part B: Neuropsychiatric Genetics* 156, 700-708 (2011).
48. Davies MN, Volta M, Pidsley R, et al. Functional annotation of the human brain methylome identifies tissue-specific epigenetic variation across brain and blood. *Genome Biology* 13, R43 (2012).
49. Hannon E, Lunnon K, Schalkwyk L, and Mill J. Interindividual methylomic variation across blood, cortex, and cerebellum: implications for epigenetic studies of neurological and neuropsychiatric phenotypes. *Epigenetics* 10, 1024-1032 (2015).
50. Yamamoto T, Toki S, Siegle GJ, et al. Increased amygdala reactivity following early life stress: a potential resilience enhancer role. *BMC Psychiatry* 17, 27 (2017).
51. Illingworth RS, Gruenewald-Schneider U, De Sousa D, et al. Inter-individual variability contrasts with regional homogeneity in the human brain DNA methylome. *Nucleic Acids Research* 43, 732-744 (2015).
52. Klengel T and Binder Elisabeth B. Epigenetics of Stress-Related Psychiatric Disorders and Gene × Environment Interactions. *Neuron* 86, 1343-1357 (2015).
53. Heim CM, Entringer S, and Buss C. Translating basic research knowledge on the biological embedding of early-life stress into novel approaches for the developmental programming of lifelong health. *Psychoneuroendocrinology* 105, 123-137 (2019).
54. Miller GE, Chen E, and Parker KJ. Psychological stress in childhood and susceptibility to the chronic diseases of aging: Moving toward a model of behavioral and biological mechanisms. *Psychological Bulletin* 137, 959-997 (2011).
55. Booij L, Szyf M, Carballedo A, et al. DNA Methylation of the Serotonin Transporter Gene in Peripheral Cells and Stress-Related Changes in Hippocampal Volume: A Study in Depressed Patients and Healthy Controls. *PLOS ONE* 10, e0119061 (2015).
56. Frodl T, Szyf M, Carballedo A, et al. DNA methylation of the serotonin transporter gene (*SLC6A4*) is associated with brain function involved in processing emotional stimuli. *Journal of Psychiatry and Neuroscience* 40, 296-305 (2015).
57. Ismaylova E, Lévesque ML, Pomares FB, et al. Serotonin transporter promoter methylation in peripheral cells and neural responses to negative stimuli: A study of adolescent monozygotic twins. *Translational Psychiatry* 8, 147 (2018).
58. Vukojevic V, Kolassa I-T, Fastenrath M, et al. Epigenetic Modification of the Glucocorticoid Receptor Gene Is Linked to Traumatic Memory and Post-Traumatic Stress Disorder Risk in Genocide Survivors. *Journal of Neuroscience* 34, 10274-10284 (2014).
59. Schechter DS, Moser DA, Paoloni-Giacobino A, et al. Methylation of NR3C1 is related to maternal PTSD, parenting stress and maternal medial prefrontal cortical activity in response to child separation among mothers with histories of violence exposure. *Frontiers in Psychology* 6, (2015).
60. Tozzi L, Farrell C, Booij L, et al. Epigenetic Changes of FKBP5 as a Link Connecting Genetic and Environmental Risk Factors with Structural and Functional Brain Changes in Major Depression. *Neuropsychopharmacology* 43, 1138-1145 (2018).
61. Sadeh N, Wolf EJ, Logue MW, et al. EPIGENETIC VARIATION AT *SKA2* PREDICTS SUICIDE PHENOTYPES AND INTERNALIZING PSYCHOPATHOLOGY: 2015 Donald F Klein Investigator Award Finalist: Epigenetic Variation at SKA2 Predicts Suicide Phenotypes. *Depression and Anxiety* 33, 308-315 (2016).
62. Sadeh N, Spielberg JM, Logue MW, et al. SKA2 methylation is associated with decreased prefrontal cortical thickness and greater PTSD severity among trauma-exposed veterans. *Molecular Psychiatry* 21, 357-363 (2016).
63. Gluck RL, Hartzell GE, Dixon HD, et al. Trauma exposure and stress-related disorders in a large, urban, predominantly African-American, female sample. *Arch Womens Ment Health* 24, 893-901 (2021).

64. Bernstein DP, Stein JA, Newcomb MD, et al. Development and validation of a brief screening version of the Childhood Trauma Questionnaire. *Child Abuse & Neglect* 27, 169-190 (2003).
65. Kilaru V, Iyer SV, Almli LM, et al. Genome-wide gene-based analysis suggests an association between Neuroligin 1 (NLGN1) and post-traumatic stress disorder. *Translational Psychiatry* 6, e820-e820 (2016).
66. Dunn EC, Nishimi K, Powers A, and Bradley B. Is developmental timing of trauma exposure associated with depressive and post-traumatic stress disorder symptoms in adulthood? *Journal of Psychiatric Research* 84, 119-127 (2017).
67. Powers A, Ressler KJ, and Bradley RG. The protective role of friendship on the effects of childhood abuse and depression. *Depression and Anxiety* 26, 46-53 (2009).
68. Binder EB. Association of FKBP5 Polymorphisms and Childhood Abuse With Risk of Posttraumatic Stress Disorder Symptoms in Adults. *JAMA* 299, 1291 (2008).
69. Stevens JS, Jovanovic T, Fani N, et al. Disrupted amygdala-prefrontal functional connectivity in civilian women with posttraumatic stress disorder. *Journal of Psychiatric Research* 47, 1469-1478 (2013).
70. Stevens JS, Kim YJ, Galatzer-Levy IR, et al. Amygdala Reactivity and Anterior Cingulate Habituation Predict Posttraumatic Stress Disorder Symptom Maintenance After Acute Civilian Trauma. *Biological Psychiatry* 81, 1023-1029 (2017).
71. Stevens JS, Reddy R, Kim YJ, et al. Episodic memory after trauma exposure: Medial temporal lobe function is positively related to re-experiencing and inversely related to negative affect symptoms. *Neuroimage Clin* 17, 650-658 (2018).
72. van Rooij SJ, Stevens JS, Ely TD, et al. Childhood Trauma and COMT Genotype Interact to Increase Hippocampal Activation in Resilient Individuals. *Front Psychiatry* 7, 156 (2016).
73. Wierenga LM, Langen M, Oranje B, and Durston S. Unique developmental trajectories of cortical thickness and surface area. *NeuroImage* 87, 120-126 (2014).
74. Panizzon MS, Fennema-Notestine C, Eyler LT, et al. Distinct Genetic Influences on Cortical Surface Area and Cortical Thickness. *Cerebral Cortex* 19, 2728-2735 (2009).
75. Ratanatharathorn A, Boks MP, Maihofer AX, et al. Epigenome-wide association of PTSD from heterogeneous cohorts with a common multi-site analysis pipeline. *American Journal of Medical Genetics Part B: Neuropsychiatric Genetics* 174, 619-630 (2017).
76. Team RC, *R: A language and environment for statistical computing*. 2019, R Foundation for Statistical Computing: Vienna, Austria.
77. Barfield RT, Kilaru V, Smith AK, and Conneely KN. CpGassoc: an R function for analysis of DNA methylation microarray data. *Bioinformatics* 28, 1280-1281 (2012).
78. McCartney DL, Walker RM, Morris SW, McIntosh AM, Porteous DJ, and Evans KL. Identification of polymorphic and off-target probe binding sites on the Illumina Infinium MethylationEPIC BeadChip. *Genomics Data* 9, 22-24 (2016).
79. Teschendorff AE, Marabita F, Lechner M, et al. A beta-mixture quantile normalization method for correcting probe design bias in Illumina Infinium 450 k DNA methylation data. *Bioinformatics* 29, 189-196 (2013).
80. Pidsley R, Y Wong CC, Volta M, Lunnon K, Mill J, and Schalkwyk LC. A data-driven approach to preprocessing Illumina 450K methylation array data. *BMC Genomics* 14, 293 (2013).
81. Du P, Zhang X, Huang C-C, et al. Comparison of Beta-value and M-value methods for quantifying methylation levels by microarray analysis. *BMC Bioinformatics* 11, 587 (2010).
82. Braun PR, Han S, Hing B, et al. Genome-wide DNA methylation comparison between live human brain and peripheral tissues within individuals. *Translational Psychiatry* 9, 47 (2019).
83. Barcelona V, Huang Y, Brown K, et al. Novel DNA methylation sites associated with cigarette smoking among African Americans. *Epigenetics* 14, 383-391 (2019).
84. Houseman EA, Accomando WP, Koestler DC, et al. DNA methylation arrays as surrogate measures of cell mixture distribution. *BMC Bioinformatics* 13, 86 (2012).
85. Purcell S, Neale B, Todd-Brown K, et al. PLINK: A Tool Set for Whole-Genome Association and Population-Based Linkage Analyses. *The American Journal of Human Genetics* 81, 559-575 (2007).
86. Meyers JL, Salling MC, Almli LM, et al. Frequency of alcohol consumption in humans; the role of metabotropic glutamate receptors and downstream signaling pathways. *Translational Psychiatry* 5, e586-e586 (2015).

87. Joehanes R, Just AC, Marioni RE, et al. Epigenetic Signatures of Cigarette Smoking. *Circulation: Cardiovascular Genetics* 9, 436-447 (2016).
88. Group tTSBS, Logue MW, Miller MW, et al. An epigenome-wide association study of posttraumatic stress disorder in US veterans implicates several new DNA methylation loci. *Clinical Epigenetics* 12, 46 (2020).
89. Langfelder P and Horvath S. WGCNA: an R package for weighted correlation network analysis. *BMC Bioinformatics* 9, 559 (2008).
90. Lin X, Barton S, and Holbrook JD. How to make DNA methylome wide association studies more powerful. *Epigenomics* 8, 1117-1129 (2016).
91. Katrinli S, Stevens J, Wani AH, et al. Evaluating the impact of trauma and PTSD on epigenetic prediction of lifespan and neural integrity. *Neuropsychopharmacology* 45, 1609-1616 (2020).
92. Luby J, Belden A, Botteron K, et al. The Effects of Poverty on Childhood Brain Development: The Mediating Effect of Caregiving and Stressful Life Events. *JAMA Pediatrics* 167, 1135 (2013).
93. Barfield R, Shen J, Just AC, et al. Testing for the indirect effect under the null for genome-wide mediation analyses. *Genetic Epidemiology* 41, 824-833 (2017).
94. Ren X and Kuan PF. methylGSA: a Bioconductor package and Shiny app for DNA methylation data length bias adjustment in gene set testing. *Bioinformatics* 35, 1958-1959 (2019).
95. Supek F, Bošnjak M, Škunca N, and Šmuc T. REVIGO Summarizes and Visualizes Long Lists of Gene Ontology Terms. *PLoS ONE* 6, e21800 (2011).
96. Segerstrom SC and Miller GE. Psychological Stress and the Human Immune System: A Meta-Analytic Study of 30 Years of Inquiry. *Psychological Bulletin* 130, 601-630 (2004).
97. Anisman H. Cascading effects of stressors and inflammatory immune system activation: implications for major depressive disorder. *J Psychiatry Neurosci* 34, 4-20 (2009).
98. Nusslock R and Miller GE. Early-Life Adversity and Physical and Emotional Health Across the Lifespan: A Neuroimmune Network Hypothesis. *Biological Psychiatry* 80, 23-32 (2016).
99. Eckart C, Stoppel C, Kaufmann J, et al. Structural alterations in lateral prefrontal, parietal and posterior midline regions of men with chronic posttraumatic stress disorder. *Journal of Psychiatry and Neuroscience* 36, 176-186 (2011).
100. Legge RM, Sendi S, Cole JH, et al. Modulatory effects of brain-derived neurotrophic factor Val66Met polymorphism on prefrontal regions in major depressive disorder. *British Journal of Psychiatry* 206, 379-384 (2015).
101. Papmeyer M, Giles S, Sussmann JE, et al. Cortical Thickness in Individuals at High Familial Risk of Mood Disorders as They Develop Major Depressive Disorder. *Biological Psychiatry* 78, 58-66 (2015).
102. Butterworth P, Cherbuin N, Sachdev P, and Anstey KJ. The association between financial hardship and amygdala and hippocampal volumes: results from the PATH through life project. *Social Cognitive and Affective Neuroscience* 7, 548-556 (2012).
103. Brito NH and Noble KG. Socioeconomic status and structural brain development. *Frontiers in Neuroscience* 8, (2014).
104. Sipahi L, Wildman DE, Aiello AE, et al. Longitudinal epigenetic variation of DNA methyltransferase genes is associated with vulnerability to post-traumatic stress disorder. *Psychological Medicine* 44, 3165-3179 (2014).
105. Lewis C. *Major Depressive Disorder Working Group of the Psychiatric Genomics Consortium*. 2020; Available from: https://www.med.unc.edu/pgc/pgc-workgroups/major-depressive-disorder/.
106. Feng J, Zhou Y, Campbell SL, et al. Dnmt1 and Dnmt3a maintain DNA methylation and regulate synaptic function in adult forebrain neurons. *Nature Neuroscience* 13, 423-430 (2010).
107. LaPlant Q, Vialou V, Covington HE, et al. Dnmt3a regulates emotional behavior and spine plasticity in the nucleus accumbens. *Nature Neuroscience* 13, 1137-1143 (2010).
108. Xu S, Sui J, Yang S, Liu Y, Wang Y, and Liang G. Integrative analysis of competing endogenous RNA network focusing on long noncoding RNA associated with progression of cutaneous melanoma. *Cancer Medicine* 7, 1019-1029 (2018).
109. Li H, Jia Y, Cheng J, Liu G, and Song F. LncRNA NCK1-AS1 promotes proliferation and induces cell cycle progression by crosstalk NCK1-AS1/miR-6857/CDK1 pathway. *Cell Death & Disease* 9, 198 (2018).
110. Mirza AH, Berthelsen CH, Seemann SE, et al. Transcriptomic landscape of lncRNAs in inflammatory bowel disease. *Genome Medicine* 7, 39 (2015).

111. Taudien S, Galgoczy P, Huse K, et al. Polymorphic segmental duplications at 8p23.1 challenge the determination of individual defensin gene repertoires and the assembly of a contiguous human reference sequence. *BMC Genomics* 5, 92 (2004).
112. Huang Y and Chen Z. Inflammatory bowel disease related innate immunity and adaptive immunity. *Am J Transl Res* 8, 2490-7 (2016).
113. Danese A, Caspi A, Williams B, et al. Biological embedding of stress through inflammation processes in childhood. *Molecular Psychiatry* 16, 244-246 (2011).
114. Baumeister D, Akhtar R, Ciufolini S, Pariante CM, and Mondelli V. Childhood trauma and adulthood inflammation: a meta-analysis of peripheral C-reactive protein, interleukin-6 and tumour necrosis factor-α. *Molecular Psychiatry* 21, 642-649 (2016).
115. Danese A, Pariante CM, Caspi A, Taylor A, and Poulton R. Childhood maltreatment predicts adult inflammation in a life-course study. *Proceedings of the National Academy of Sciences* 104, 1319-1324 (2007).
116. Patel N, Crider A, Pandya CD, Ahmed AO, and Pillai A. Altered mRNA Levels of Glucocorticoid Receptor, Mineralocorticoid Receptor, and Co-Chaperones (FKBP5 and PTGES3) in the Middle Frontal Gyrus of Autism Spectrum Disorder Subjects. *Molecular Neurobiology* 53, 2090-2099 (2016).
117. Sinclair D, Tsai SY, Woon HG, and Weickert CS. Abnormal Glucocorticoid Receptor mRNA and Protein Isoform Expression in the Prefrontal Cortex in Psychiatric Illness. *Neuropsychopharmacology* 36, 2698-2709 (2011).
118. Sinclair D, Fillman SG, Webster MJ, and Weickert CS. Dysregulation of glucocorticoid receptor co-factors FKBP5, BAG1 and PTGES3 in prefrontal cortex in psychotic illness. *Scientific Reports* 3, 3539 (2013).
119. Meier TB, Drevets WC, Wurfel BE, et al. Relationship between neurotoxic kynurenine metabolites and reductions in right medial prefrontal cortical thickness in major depressive disorder. *Brain, Behavior, and Immunity* 53, 39-48 (2016).
120. Gresset A, Sondek J, and Harden TK, *The Phospholipase C Isozymes and Their Regulation*, in *Phosphoinositides I: Enzymes of Synthesis and Degradation*, Balla T, Wymann M, and York JD, Editors. 2012, Springer Netherlands: Dordrecht. p. 61-94.
121. Hu X-T, Zhang F-B, Fan Y-C, et al. Phospholipase C delta 1 is a novel 3p22.3 tumor suppressor involved in cytoskeleton organization, with its epigenetic silencing correlated with high-stage gastric cancer. *Oncogene* 28, 2466-2475 (2009).
122. Ichinohe M, Nakamura Y, Sai K, Nakahara M, Yamaguchi H, and Fukami K. Lack of phospholipase C-δ1 induces skin inflammation. *Biochemical and Biophysical Research Communications* 356, 912-918 (2007).
123. Stallings JD, Tall EG, Pentyala S, and Rebecchi MJ. Nuclear Translocation of Phospholipase C-δ1 Is Linked to the Cell Cycle and Nuclear Phosphatidylinositol 4,5-Bisphosphate. *Journal of Biological Chemistry* 280, 22060-22069 (2005).
124. Yu H, Fukami K, Watanabe Y, Ozaki C, and Takenawa T. Phosphatidylinositol 4,5-bisphosphate reverses the inhibition of RNA transcription caused by histone H1. *European Journal of Biochemistry* 251, 281-287 (1998).
125. Haddad JJ, Saadé NE, and Safieh-Garabedian B. Cytokines and neuro–immune–endocrine interactions: a role for the hypothalamic–pituitary–adrenal revolving axis. *Journal of Neuroimmunology* 133, 1-19 (2002).
126. Sternberg EM. Neural regulation of innate immunity: a coordinated nonspecific host response to pathogens. *Nature Reviews Immunology* 6, 318-328 (2006).
127. Vilsaint CL, NeMoyer A, Fillbrunn M, et al. Racial/ethnic differences in 12-month prevalence and persistence of mood, anxiety, and substance use disorders: Variation by nativity and socioeconomic status. *Comprehensive Psychiatry* 89, 52-60 (2019).

991

Table 1. Demographic & psychosocial measure summary statistics (non-scaled) for the current sample (n = 97)

Measure	Description	Value
Age	Mean [SD] (Range)	40 [12.5] (19 - 62)
Sex	Female	100%
Self-reported race/ethnicity	African American	100%
Household income (income)	$0-499	30%
	$499-999	36%
	$1000+	34%
Educational attainment (education)	Some high school	15%
	High school grad or GED	30%
	≥ Undergraduate degree	55%
Employment/disability	Employed	33%
	Disabled (not employed)	7%
	Not employed or disabled	60%
Childhood trauma questionnaire (CTQ total)	Mean [SD] (Range)	40.5 [15.4] (25 - 93)
Traumatic events inventory (TEI)	Mean [SD] (Range)	4.2 [2.3] (0 - 10.7)

Legend: [standard deviation], (range).

Table 2. Adverse social exposures (ASEs) predict hemisphere-mean fronto-limbic brain morphometry

	Low household income				Low educational attainment				Childhood trauma burden				Adult trauma burden			
	β	**SE**	**T**	**P**	**β**	**SE**	**T**	**P**	**β**	**SE**	**T**	**P**	**β**	**SE**	**T**	**P**
Hipp. Volume (mm3)	-0.425	0.267	-1.590	0.116	0.005	0.279	0.019	0.985	0.030	0.115	0.260	0.796	-0.167	0.101	-1.644	0.104
Amyg. Volume (mm3)	-0.649	0.283	-2.299	0.024*	0.091	0.294	0.310	0.757	0.145	0.118	1.228	0.223	-0.146	0.106	-1.380	0.171
FP SA (mm2)	0.556	0.285	1.950	0.055	-0.065	0.294	-0.221	0.826	-0.004	0.114	-0.037	0.971	0.109	0.107	1.017	0.312
Medial OFC SA (mm2)	0.271	0.293	0.926	0.357	-0.374	0.302	-1.237	0.220	-0.052	0.117	-0.440	0.661	-0.112	0.110	-1.021	0.310
Lateral OFC SA (mm2)	-0.033	0.298	-0.111	0.912	-0.244	0.307	-0.796	0.428	-0.211	0.119	-1.769	0.081	-0.093	0.111	-0.834	0.407
SFG SA (mm2)	0.386	0.289	1.336	0.185	-0.435	0.298	-1.460	0.148	-0.223	0.116	-1.926	0.058	0.039	0.108	0.358	0.721
RMFG SA (mm2)	-0.050	0.278	-0.181	0.857	-0.543	0.286	-1.897	0.061	-0.231	0.111	-2.079	0.041*	0.036	0.104	0.346	0.730
Rostral ACC SA (mm2)	-0.176	0.291	-0.602	0.549	-0.511	0.301	-1.700	0.093	-0.229	0.117	-1.961	0.053	0.029	0.109	0.268	0.790
Caudal ACC SA (mm2)	0.121	0.272	0.443	0.659	-0.855	0.280	-3.049	0.003**	-0.110	0.109	-1.006	0.317	0.044	0.102	0.436	0.664
FP CT (mm)	-0.137	0.293	-0.468	0.641	0.684	0.302	2.267	0.026*	-0.079	0.117	-0.671	0.504	-0.120	0.110	-1.098	0.275
Medial OFC CT (mm)	-0.002	0.293	-0.008	0.993	0.346	0.315	1.099	0.275	0.138	0.118	1.172	0.244	0.022	0.111	0.202	0.840
Lateral OFC CT (mm)	-0.023	0.304	-0.074	0.941	0.241	0.314	0.769	0.444	0.055	0.122	0.451	0.653	-0.112	0.114	-0.983	0.328
SFG CT (mm)	-0.088	0.248	-0.356	0.723	0.553	0.256	2.162	0.034*	0.070	0.100	0.699	0.487	-0.170	0.093	-1.831	0.071
RMFG CT (mm)	-0.078	0.281	-0.276	0.783	0.443	0.290	1.530	0.130	0.072	0.113	0.637	0.526	-0.112	0.105	-1.062	0.291
Rostral ACC CT (mm)	-0.063	0.297	-0.211	0.833	0.060	0.318	0.188	0.851	0.019	0.118	0.163	0.871	-0.034	0.112	-0.305	0.761
Caudal ACC CT (mm)	-0.124	0.296	-0.419	0.676	0.187	0.318	0.589	0.558	0.046	0.119	0.388	0.699	0.004	0.112	0.039	0.969

*** P < 0.001, **P < 0.01, * P < 0.05, **P: BH significant (bold)**

Both dependent and independent variables were scaled prior to analysis. Childhood trauma burden was measured with the Childhood Trauma Questionnaire, and adult trauma burden was measured with the Traumatic Events Inventory. In separate linear models including hippocampus and amygdala volumes as dependent variables, income, education, CTQ total, and TEI were included as independent variables of interest, whereas genomic ancestry, age, employment/disability and ICV were included as covariates. The same independent variables and covariates were included, minus ICV, to predict frontal cortex subregions SA and CT measures.

Abbreviations. Hipp: hippocampus, Amyg: amygdala, FP: frontal pole, mOFC: medial orbito-frontal cortex, lOFC: lateral orbito-frontal cortex, SFG: superior frontal gyrus, RMFG: rostral medial frontal gyrus, rACC: rostral anterior cingulate cortex, cACC: caudal anterior cingulate cortex, SA: surface area, CT: cortical thickness, β: scaled beta value, SE: standard error, T: t statistic value.

Table 3. Module eigengenes (MEs) mediating observed adverse social exposure (ASE), fronto-limbic brain morphometry relationships

Maroon: Rostral Mid Frontal Gyrus SA		β	95% CI Lower	95% CI Upper
	Average indirect effect (IDE)	**-0.466****	-0.952	-0.098
	Average direct effect (DE)	-0.517	-1.464	0.407
	Average total effect (TE)	-0.983*	-1.959	-0.016
Tan: Rostral Mid Frontal Gyrus SA		β	95% CI Lower	95% CI Upper
	Average indirect effect (IDE)	-0.124	-0.448	0.100
	Average direct effect (DE)	-0.884	-1.869	0.085
	Average total effect (TE)	-1.001*	-1.955	-0.040
White: Rostral Mid Frontal Gyrus SA		β	95% CI Lower	95% CI Upper
	Average indirect effect (IDE)	**-0.348***	-0.781	-0.026
	Average direct effect (DE)	-0.667	-1.590	0.251
	Average total effect (TE)	-1.014*	-1.983	-0.069
Yellow: Rostral Mid Frontal Gyrus SA		β	95% CI Lower	95% CI Upper
	Average indirect effect (IDE)	-0.128	-0.474	0.142
	Average direct effect (DE)	-0.888	-1.908	0.148
	Average total effect (TE)	-1.016*	-2.003	-0.019
Lightcoral: Caudal ACC SA		β	95% CI Lower	95% CI Upper
	Average indirect effect (IDE)	-0.107	-0.307	0.015
	Average direct effect (DE)	**-0.737***	-1.296	-0.176
	Average total effect (TE)	-0.844**	-1.394	-0.283

*** P < 0.001, ** P < 0.01, * P < 0.05, **P: BH-significant (bolded)**

Both dependent and independent variables were scaled prior to analysis. SA: surface area (mm2), CT: cortical thickness (mm), β: coefficient estimate, CI: confidence interval

Table 4. Probe-wise mediation analysis of the relationship between childhood trauma burden (CTQ total) & rostral middle frontal gyrus (RMFG) surface area (SA)

Probe name	Module name	Chr:pos (hg38)	Gene name	IDE β	IDE P	DE β	DE P	TE β	TE P
cg21622733	**Maroon**	Chr19:35408551	*LINC01531*	**-0.512**	**0.003****	-0.471	0.320	-0.983	0.044*
cg19805668	**Maroon**	Chr14:74951972	*PGF*	**-0.411**	**0.009****	-0.592	0.217	-1.003	0.042*
cg10592766	Maroon	Chr19:50226846	*MYH14*	-0.321	0.019*	-0.670	0.182	-0.990	0.048*
cg03710029	Maroon	Chr17:81291801	*SLC38A10*	-0.383	0.025*	-0.613	0.188	-0.996	0.043*
cg15150970	Maroon	Chr2:25250660	*DNMT3A*	-0.253	0.049*	-0.753	0.125	-1.006	0.040*
cg12219789	Maroon	Chr17:7324180	*NEURL4*	-0.352	0.049*	-0.622	0.183	-0.974	0.049*
cg01544227	White	Chr12:8323720	*AC092745.5*	-0.305	0.036*	-0.689	0.175	-0.994	0.044*
cg00686169	White	Chr8:8024026	*FAM90A24P*	-0.277	0.043*	-0.740	0.126	-1.017	0.037*
cg08002107	White	Chr8:12135255	*USP17L7*	-0.268	0.047*	-0.738	0.122	-1.006	0.040*

*** P < 0.001, **P < 0.01, * P < 0.05, **P: BH-significant (bold)**

Both dependent and independent variables were scaled prior to analysis. IDE: indirect effect, DE: direct effect, TE: total effect, β: coefficient estimate, P: nominal p-value, BH: Benjamini-Hochberg

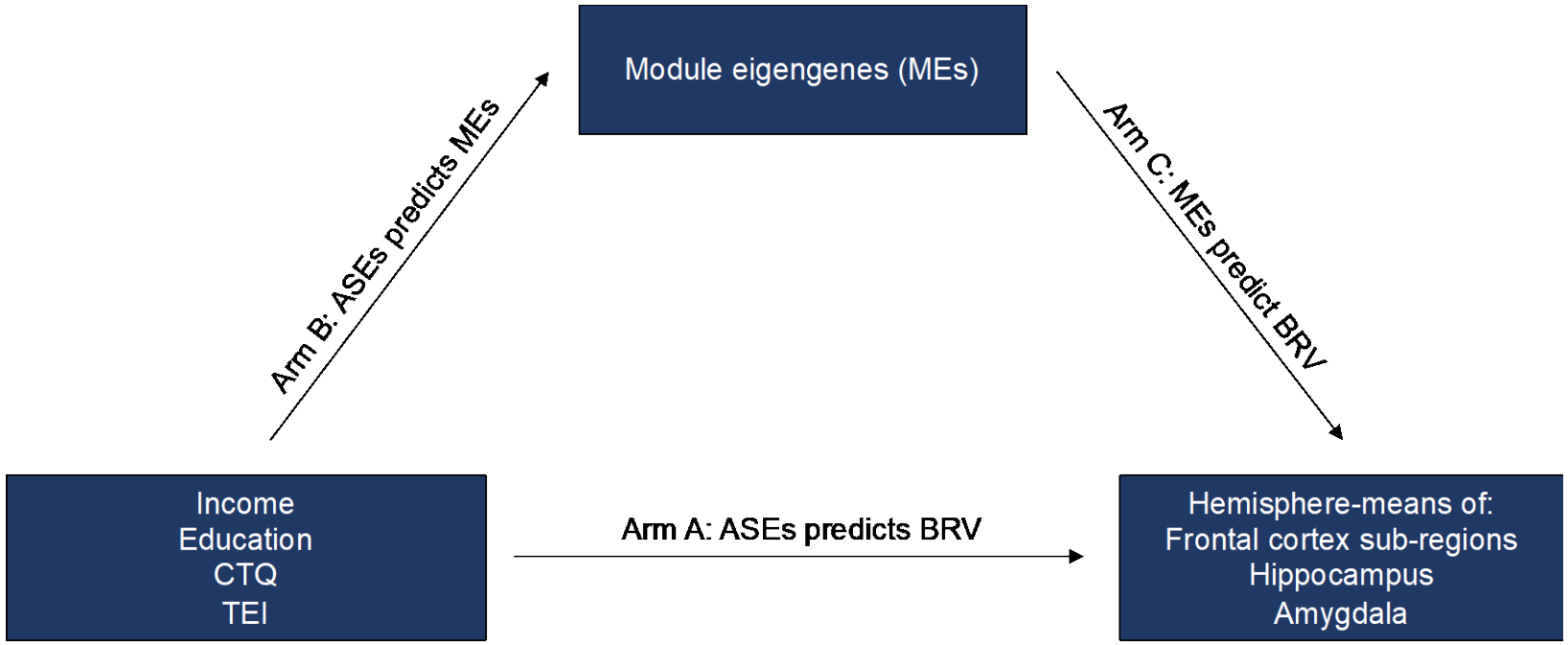

Figure 1. Conceptual model testing individual module eigengenes (MEs) as mediators of the hypothesized associations between adverse social exposures (ASEs) and variability in fronto-limbic brain morphometries. Arm A. Analyses included hemisphere-mean hippocampus and amygdala volumes as dependent variables (in separate models). Income, education, CTQ total, and TEI were included as independent variables of interest, whereas genomic ancestry, age, employment/disability and ICV were included as covariates. The same predictors and covariates were included, minus ICV, to predict frontal cortex subregions SA and CT measures. Arm B. Analyses included 5mC MEs as dependent variables (in separate models). Income, education, CTQ total, and TEI were included as independent variables of interest, and employment/disability was included as a covariate. Arm C. Analyses included individual fronto-limbic morphometry measures as dependent variables (in separate models). Individual 5mC MEs were included as independent variables of interest, whereas age, genomic ancestry, employment, and ICV (ICV was only included in hippocampus and amygdala models) were included as covariates.

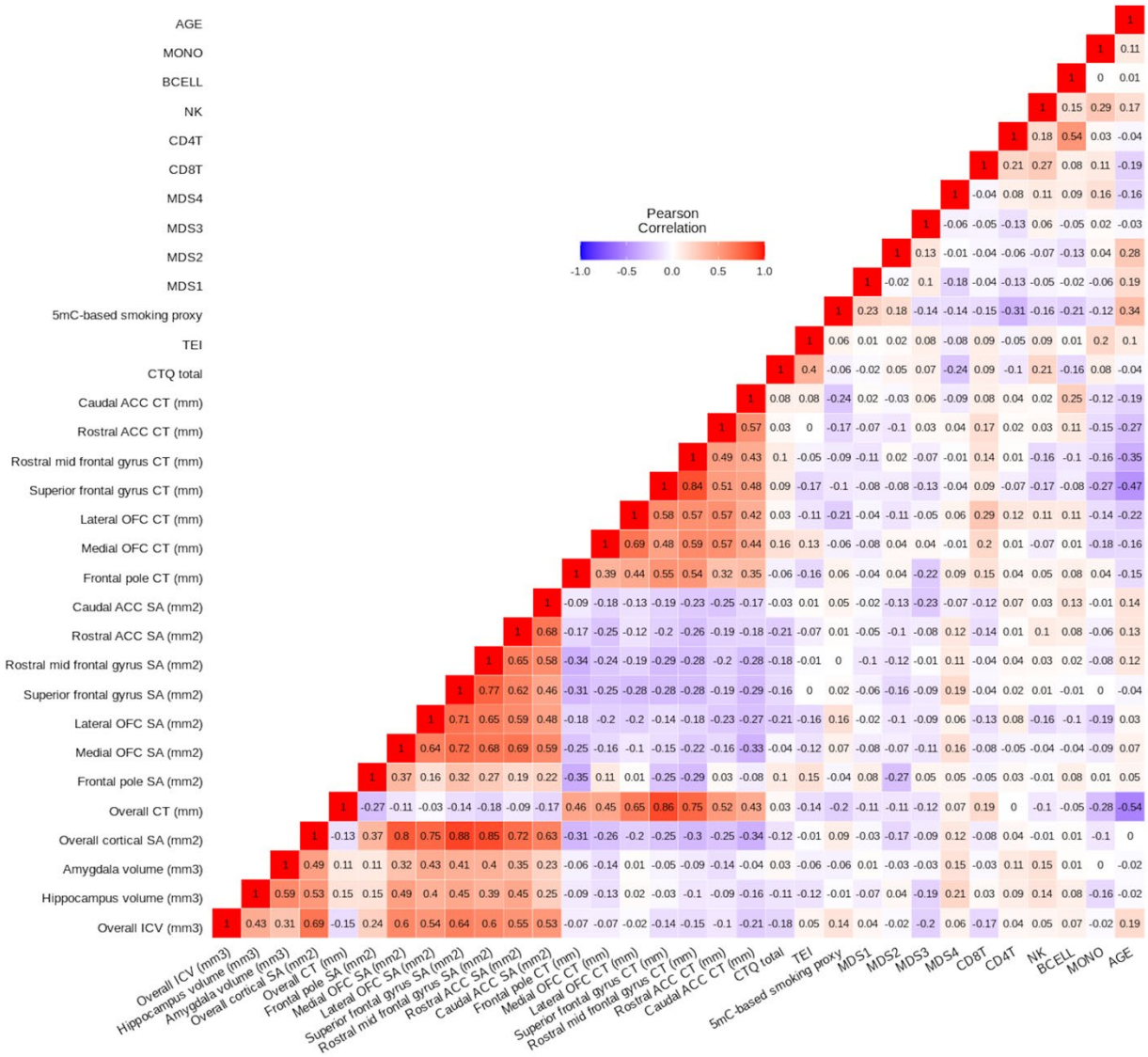

Figure 2. Pearson's correlation heatmap of variables used throughout the current study. Age is negatively associated with multiple frontal cortex cortical thickness (CT) measures (Pearson's correlation r_{range} = -0.15 to -0.47, p_{range} = 0.092 to $6x10^{-7}$). Within frontal cortex CT measures, multiple subregions show positive correlations with one another (Pearson's correlation r_{range} = 0.32 to 0.84, p_{range} = 0.004 to < $2x10^{-16}$). The same phenomenon is observed within frontal cortex surface area (SA) measures (Pearson's correlation r_{range} = 0.16 to 0.77, p_{range} = 0.210 to <$2x10^{-16}$). Overall CT is positively correlated with each of the frontal cortex CT measures (Pearson's correlation r_{range} = 0.43 to 0.86, p_{range} = $1x10^{-7}$ to <$2x10^{-16}$), and overall SA is positively correlated with each of the frontal cortex SA measures (Pearson's correlation r_{range} = 0.37 to 0.88, p_{range} = $5x10^{-4}$ to < $2x10^{-16}$).

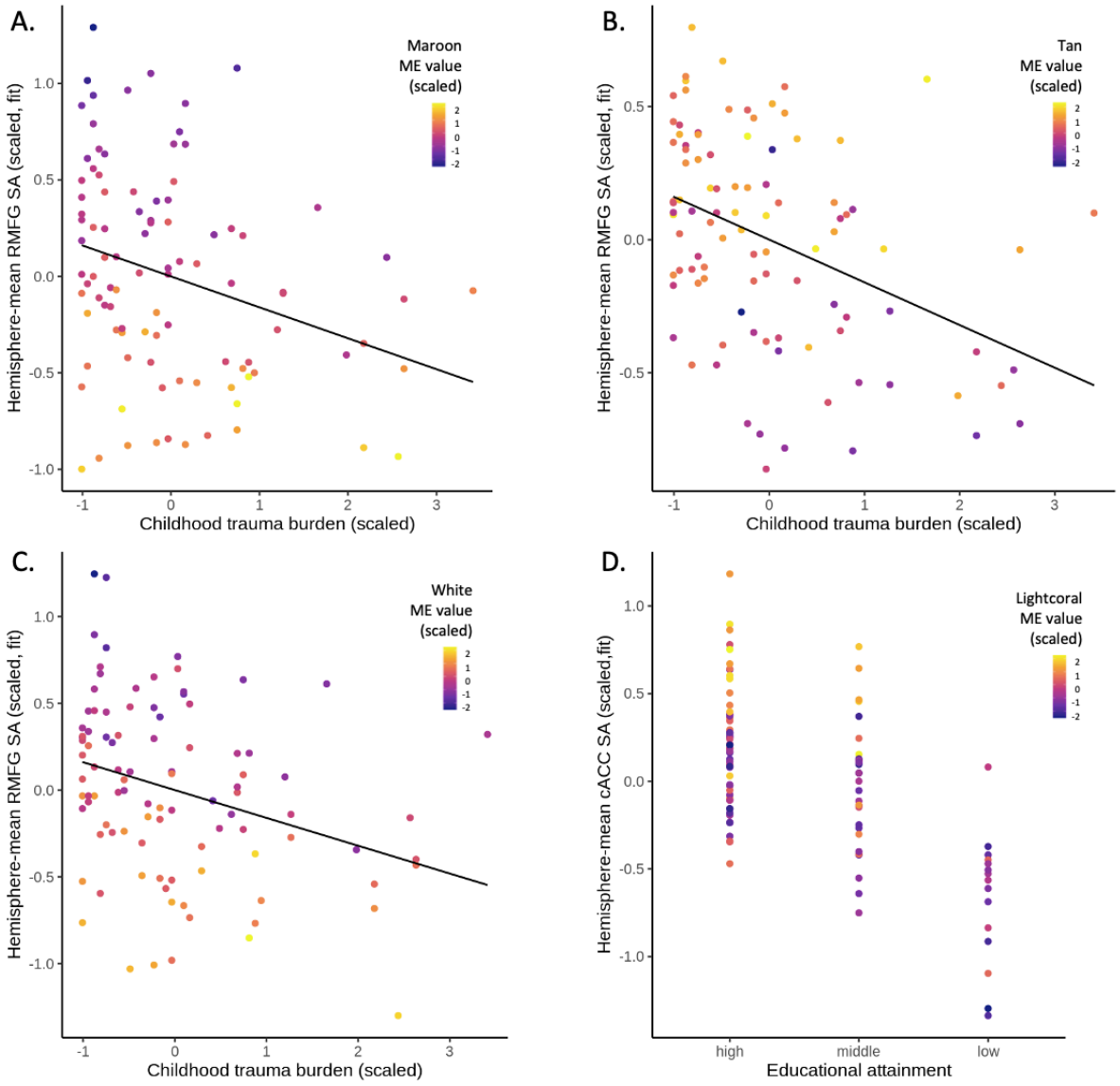

Figure 3. CTQ total is negatively associated with rostral middle frontal gyrus (RMFG) surface area (SA). Low educational attainment status is associated with low caudal anterior cingulate cortex (cACC) SA. Out of seven CTQ-associated module eigengenes (MEs), the three strongest relationships with hemisphere-mean RMFG SA were the Maroon (A), White (B), and Tan (C) MEs. Out of two low education attainment-associated MEs, the strongest relationship with hemisphere-mean cACC SA was the Lightcoral ME (D). As shown, neuroimaging measures are adjusted by age, ME value, genomic ancestry, employment/disability status, and an adverse social exposure (ASE). Dependent and independent variables were scaled. A. CTQ total was positively associated with the Maroon ME ($\beta = 0.289$, SE = 0.109, $t = 2.639$, $p = 9.8 \times 10^{-3}$). In turn, the Maroon ME was negatively associated with RMFG SA ($\beta = -0.451$, SE = 0.091, $t = -4.966$, $p = 3 \times 10^{-6}$). B. CTQ total was negatively associated with the Tan ME ($\beta = -0.248$, SE = 0.112, $t = -2.220$, $p = 0.029$). The Tan ME was, in turn, positively associated with RMFG SA ($\beta = 0.233$, SE = 0.100, $t = 2.322$, $p = 0.023$). C. CTQ total was positively associated with the White ME ($\beta = 0.236$, SE = 0.110, $t = 2.151$, $p = 0.034$). In turn, the White ME was negatively associated with RMFG SA ($\beta = -0.392$, SE = 0.093, $t = -4.231$, $p = 6 \times 10^{-5}$). D. Low educational attainment (no high school certificate) was associated with the Lightcoral ME ($\beta = -0.615$, SE = 0.296, $t = -2.079$, $p = 0.040$). The Lightcoral ME, in turn, was positively associated with cACC SA ($\beta = 0.215$, SE = 0.099, $t = 2.182$, $p = 0.032$).